

# Immobilization of Alpha-Amylase onto Ni<sup>2+</sup> Attached Carbon Felt: Investigation of Kinetic Parameters from Potato Wastewater

Ömür Acet, Tülden İnanan, Eda Ondul Koc, Buse Sert, Burcu Önal Acet, Mehmet Odabaşı, Kasim Ocakoglu, and Nadir Dizge\*

$\alpha$ -amylase is an important enzyme for textile, food, paper, and the pharmaceutical industrial areas. In this study, Ni<sup>2+</sup> attached carbon felt structures with nitrogen active site (Ni<sup>2+</sup>-N-ACF) are produced. The surface morphologies of the N-ACF and Ni<sup>2+</sup>-N-ACF are investigated by means of scanning electron microscopy (SEM) analysis. Ni<sup>2+</sup> ions binding on the N-ACFs are determined by energy dispersive X-ray (EDX) analysis and a graphite furnace atomic absorption spectrometer (AAS). The effect of pH, ionic strength, initial  $\alpha$ -amylase concentration, and temperature parameters is investigated for  $\alpha$ -amylase immobilization on Ni<sup>2+</sup>-N-ACF structures. In addition, pH and temperature effect on the activities of the free and the immobilized amylase, kinetic parameters, storage, and operational stabilities are made. Lastly, starch degradation in potato waste water is tested on Ni<sup>2+</sup>-N-ACF. The obtained results show that  $\alpha$ -amylase immobilized Ni<sup>2+</sup>-N-ACF can be used for starch degradation on an industrial scale.

## 1. Introduction

Today, the scientific world focuses on environmentally friendly, low-cost, and sustainable alternative techniques that effectively remove environmental pollutants. To this end, it seems logical to develop new, effective, greener, and hybrid strategies for removing toxic pollutants with the help of enzymes. Immobilization of enzymes is a biotechnological tool in which enzymes are fixed on the support material to increase stability and maintain structural conformation. Recyclability and reusability are the main advantages of immobilized enzymes over free enzymes.<sup>[1]</sup>

Enzymes find many implementations in various industries<sup>[2]</sup> such as the degradation of pollutants,<sup>[3]</sup> biofuel production,<sup>[4]</sup>

and bio-product recovery.<sup>[5]</sup> The replacement of chemicals with enzymes in the wet processing in some industries has been necessary process. Chemical desizing method makes hazardous effluents and this can lead to higher investments especially wastewater treatment in industry.<sup>[2]</sup> Enzymatic desizing utilizing  $\alpha$ -amylase (E.C. 3.2.1.1) has some benefits such as having a non-toxic by-product, decreased water and energy consumption,<sup>[6]</sup>  $\alpha$ -amylases are the earliest and all-purpose starch hydrolyzing enzymes which may replace chemical hydrolysis of starch in industry. They cleave the  $\alpha$ -(1,4)-D-glucosidic linkage of starch and other related polysaccharides to yield simple sugars like glucose, maltose, and limit dextrin. And also, they account for approximately 30% of the total enzyme market.<sup>[7]</sup>

Affinity chromatography techniques take place wide implementations among all classic purification methods due to less purification steps.<sup>[8–10]</sup> Lately, immobilized metal affinity chromatography (IMAC) has been generally selected for the purification of biomolecules because of its excellent features such as low cost, high biomolecule adsorption capability, and great chemical stability. These characteristics are very important for large-ratio purification in industrial practises.<sup>[11]</sup> IMAC depends upon coordination between chelated metal ions and functional groups of surface accessible amino acids, i.e., histidine (his) and cysteine (cys).<sup>[12]</sup> Metal ion immobilization on some adsorbents may enhance the interaction of them with biomolecules, which is desired for applications in IMAC.<sup>[9]</sup> It has been reported in the literature that glutamate and aspartate also contribute to the

Ö. Acet

Vocational School of Health Science  
Pharmacy Services Program  
Tarsus University  
Tarsus 33400, Turkey

T. İnanan

Technical Sciences Vocational School  
Aksaray University  
Aksaray 68100, Turkey

E. O. Koc

Yenicaga Yasar Celik Vocational School  
Bolu Abant İzzet Baysal University  
Bolu 14300, Turkey

B. Sert, K. Ocakoglu

Department of Engineering Fundamental Sciences, Faculty of Engineering  
Tarsus University  
Tarsus 33400, Turkey

B. Önal Acet, M. Odabaşı

Chemistry Department  
Faculty of Arts and Science  
Aksaray University  
Aksaray 68100, Turkey

N. Dizge

Department of Environmental Engineering  
Mersin University  
Mersin 33343, Turkey  
E-mail: nadirdizge@gmail.com

 The ORCID identification number(s) for the author(s) of this article can be found under <https://doi.org/10.1002/star.202300033>

DOI: 10.1002/star.202300033

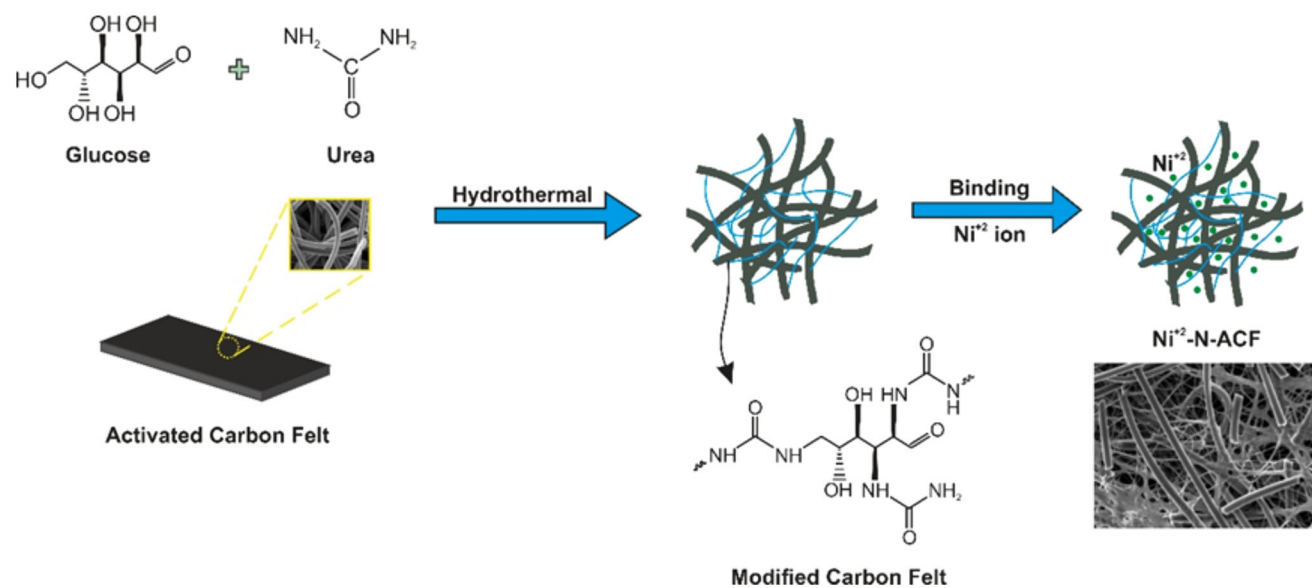


**Figure 1.** Schematic illustration for the preparation process of N-ACF and Ni<sup>2+</sup>-N-ACF.

binding, as well as proteins with amino acids that can be widely used in the IMAC process and can be reached on the surface. Even though the IMAC technique is active with His and/or Cys rich proteins in a certain pH range (6.0–8.0), the presence of amino acids such as glutamate and aspartate also offers the opportunity for IMAC to work below these pHs. Therefore, it ensures the opportunity to act as a pseudo-anion exchanger. It also has some advantages such as high-scale purification and high selectivity for biomolecules, with medium adjustment such as pH and ionic strength. This setting of media generally allows for one-step purification.<sup>[13,14]</sup>

Here, we utilized a new kind of functional, low-cost, handy, and reusable carbon felt (CF) for immobilization of  $\alpha$ -amylase. For this aim, nitrogen groups were attached on CF structures (N-ACF). Then, Ni<sup>2+</sup> ions were immobilized on N-ACF (Ni<sup>2+</sup>-N-ACF). Characterization studies were also carried out with structural analyzes (SEM) and metal binding confirmations (EDX and AAS). The effect of pH, ionic strength, initial  $\alpha$ -amylase concentration, and temperature on immobilization of  $\alpha$ -amylase on N-ACF were investigated. In addition, the effect of pH and temperature on the activity characters of free and immobilized  $\alpha$ -amylase was investigated, and their kinetic parameters, thermal, operational and storage stability were also determined.

## 2. Experimental Section

### 2.1. Materials

3,5-dinitrosalicylic acid (DNSA), starch, sodium–potassium tartrate, and  $\alpha$ -amylase were provided by Novozyme (Denmark). Activated carbon fabric was kindly provided by Norm Technologies, Turkey. The rest of chemicals were purchased at reagent grade from Merck AG (Darmstadt, Germany).

### 2.2. Preparation of Nitrogen Modified ACF (N-ACF)

ACF was treated as follows: certain amounts of glucose (5 mg) and urea (10 mg) were dissolved in distilled water (25 mL), and the mixture was transferred to a Teflon-lined autoclave. Then, the autoclave was transferred to an oven and kept at 180 °C for 6 h (Figure 1). The sample was washed with deionized water after cooling down in the open air, and it was then dried for 6 h in a vacuum oven at 70 °C.

### 2.3. Binding of Ni<sup>2+</sup> ions to N-ACF (Ni<sup>2+</sup>-N-ACF)

Binding of Ni<sup>2+</sup> ions to N-ACF was carried out (at room temperature for 2 h) with a Ni<sup>2+</sup> solution (100 ppm, pH 5.0 tuned up with 0.01 M HCl). The quantity of binded Ni<sup>2+</sup> ions onto N-ACF materials were determined with beginning and last solutions of Ni<sup>2+</sup> ion by a graphite furnace atomic absorption spectrometer (GFAAS, Analyst 800/PerkinElmer, Waltham, MA, USA).

### 2.4. Characterization Studies

Scanning electron microscopy (SEM, FEI, Ouanta FEG 250, the Netherlands) was used to characterize surface morphology of free and immobilized enzyme on ACF.

### 2.5. Adsorption and Desorption Experiments from Aqueous Solution

Adsorption studies were applied to demonstrate the impact of various experimental conditions. A rotator system (Stuart SB3) was utilized for all adsorption and elution steps.  $\alpha$ -Amylase adsorption experiments onto Ni<sup>2+</sup>-N-ACF were carried out with a

gentle rotation at 20 rpm for 30 min in various buffer systems. Adsorption studies were conducted in the range of pH 4.0–8.0 by using 0.05 M acetate buffer from pH 4.0 to 6.0. 0.05 M phosphate buffer was used for pH 7.0–8.0.  $\alpha$ -Amylase adsorption studies onto Ni<sup>2+</sup>-N-ACF materials were monitored at 280 nm and ideal conditions were investigated with some factors such as pH (4.0–8.0), initial  $\alpha$ -amylase concentration (0.25–3 mg mL<sup>-1</sup>), temperature (5–55 °C), and salt concentration effects (0–1.5 M NaCl).  $\alpha$ -Amylase adsorbed Ni<sup>2+</sup>-N-ACF materials were subjected to 1 M NaCl solution for elution of  $\alpha$ -amylase at a rotation rate of 20 rpm for 30 min. The percentage of  $\alpha$ -amylase eluted from Ni<sup>2+</sup>-N-ACF materials was ensured between adsorbed and eluted  $\alpha$ -amylase amounts.

## 2.6. Activity Experiments for the Free and the Immobilized Amylase

$\alpha$ -Amylase activity was specified according to the method of Bernfeld.<sup>[15]</sup> The assay contains spectrophotometric assay of maltose released from substrate by reducing with 3,5-dinitrosalicylic acid (DNSA). The free and the immobilized enzyme were reacted with starch solution (1%) for 3 min. The reaction was stopped by adding the DNSA solution which contains sodium-potassium tartarate (100 mM), NaOH (400 mM), and DNSA (4.4 mM). After DNSA addition, reaction solution was incubated in boiling water for 5 min and fastly cooled. The assay solution was diluted with distilled water and the intensity of colored complex was determined with a UV-spectrophotometer (Thermo Scientific GENESYS 10S UV/vis spectrophotometer) at 540 nm. Calibration curve was formed using maltose solutions at various concentrations (0.1–1.0 mM) for making decision of the released maltose. One  $\alpha$ -amylase activity unit is defined as the amount of maltose released by mg  $\alpha$ -amylase per min under specified conditions (25 °C and pH 6.9).

The immobilization of enzymes onto solid supports altered the behaviors by pH and temperature.<sup>[16]</sup> Activities of the free and the immobilized  $\alpha$ -amylase were determined in the range of pH 4.0–8.0 to determine the effect of pH on enzyme activity. For the determination of the effect of temperature, enzyme activities were investigated between 5 and 55 °C. Maximum activity for each parameter was stated as 100% and the other values were presented as relative activity percent. Kinetic parameters were calculated from Lineweaver–Burk plot which formed by different starch solutions (0.2–2.0%).

## 2.7. Storage and Operational Stabilities

Immobilization may be the key for the optimization of the operational performance for an enzyme in industrial processes.<sup>[17]</sup> Storage stabilities of the free and the immobilized  $\alpha$ -amylase were investigated periodically during 1 month. The free and the immobilized  $\alpha$ -amylase were stored at 4 °C and the activity assays were measured using 1% starch by DNSA assay. To determine operational stability, the same  $\alpha$ -amylase immobilized Ni<sup>2+</sup>-N-ACF was used 15-times at activity assay by DNSA assay and washed with pH 5.0 buffer solution between the activity runs.

## 2.8. Starch Degradation in Real Potato Wastewater

Potato wastewater was obtained from local fabric in Mersin. The starch concentration of waste water was determined as 100 ± 10 mg L<sup>-1</sup>. Blurry wastewater was filtered and the supernatant solution was directly mixed with  $\alpha$ -amylase immobilized Ni<sup>2+</sup>-N-ACF and free amylase. Some of degradation solution was taken and mixed with DNSA assay. The amount of liberated maltose by immobilized  $\alpha$ -amylase onto Ni<sup>2+</sup>-N-ACF was measured and compared with that by free  $\alpha$ -amylase.

# 3. Results and Discussion

## 3.1. Characterization Studies

Quantity of bound Ni<sup>2+</sup> ions on NH<sub>2</sub>-ACF was calculated to be 28 mg g<sup>-1</sup> N-ACF. Practiced experiments after washing showed no Ni<sup>2+</sup> ions leakage from Ni<sup>2+</sup>-N-ACF.

The surface morphologies of the samples were investigated by means of SEM analysis. The detailed SEM images taken at 200× and 1000× magnification were presented in **Figure 2**. As seen from the micrographs, the active carbon felt possessed the long fibrillose micro structure having about 15 μm width, **Figure 2A**. Moreover, when examining the **Figure 2B**, it was observed that  $\alpha$ -amylase surrounded the active carbon felt by forming the porous and flexible network appearance. This revealed that  $\alpha$ -amylase successfully immobilized on the active carbon felt including Ni metal and, the original microstructure of the active carbon felt conserved during immobilization without any deformation.

Further confirmation of Ni<sup>2+</sup> loading on the N-ACF was followed by energy dispersive X-ray (EDX) analysis. The analysis results of both null carbon felt and Ni<sup>2+</sup>-N-ACF are illustrated in **Figure 3**. The EDX pattern (**Figure 3A**) for the null carbon felt did not show the characteristic signal of Ni<sup>2+</sup>, whereas for Ni<sup>2+</sup>-N-ACF (**Figure 3B**) a clear signal of the presence of Ni<sup>2+</sup> was observed. Furthermore, the presence of Na and Cl, which have been shown in the EDX spectrum, originated from the chemicals.

FTIR spectra of bare and modified carbon felt (ACF and NH<sub>2</sub>-ACF) are shown in **Figure 4**. Only three absorption peaks were found in the spectra of the unmodified ACF at approximately 1647, 2333, and 3454 cm<sup>-1</sup>, respectively. The stretching vibrations of the –OH and H<sub>2</sub>N– groups, which both make the dots hydrophilic and improve their stability and dispersability in water, are attributed to the absorption bands at 3000–3500 cm<sup>-1</sup>. The peak at 1640 cm<sup>-1</sup> was attributed to the N–H absorption peak. Peak intensity after the modification of ACF, changed at 1053, 1650, and 3456 cm<sup>-1</sup>, indicating an increase in sp<sup>3</sup>-hybridized carbon and hence an increase in felt surface defects during modification. Furthermore, the vibrational peaks of the oxygen-containing functional groups appear to increase significantly after the felt modification. This suggests that acidic oxygen-containing functional groups, including carboxyl, hydroxyl, and carbonyl groups, penetrate the surface.

## 3.2. Adsorption and Desorption Experiments from Aqueous Solution

Adsorption of  $\alpha$ -amylase was quietly influenced by pH of the solution medium (**Figure 5A**). As a result of experiments to

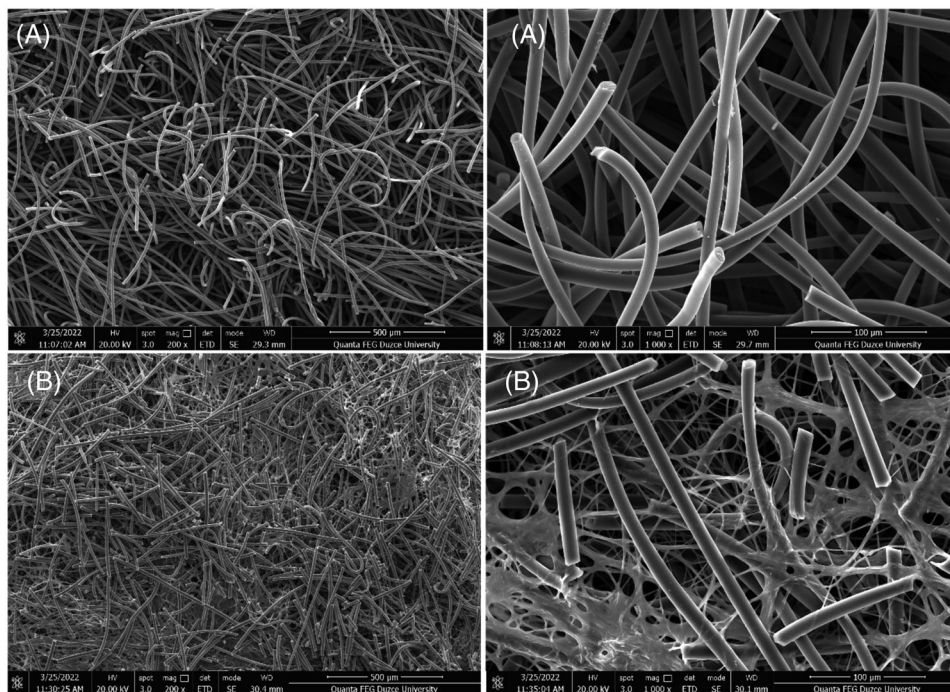


**Figure 2.** A) SEM micrographs of ACF and B) Ni<sup>2+</sup>-N-ACF including  $\alpha$ -amylase with 200 $\times$  and 1000 $\times$  magnification.

investigate the effect of pH on the adsorption capacity, the optimum pH value for  $\alpha$ -amylase with maximum adsorption capacity was found to be pH 5.0. A significant decrease was observed in the adsorption properties of the materials as the pH increased or decreased due to the repulsion between the charged  $\alpha$ -amylase. The highest adsorption capacity has been observed to occur when the pH reaches 5.0. This condition may be clarified in the literature as follows:  $\alpha$ -amylase mostly contains acidic amino acids (i.e., aspartate and glutamate) because its isoelectric point is close to the acidic region.<sup>[11,18]</sup>

It was become aware of that IMAC matrix may interact with proteins even if without the existence of IMAC active amino acid residues (i.e., histidine, cysteine) near the surface for metal-

ligand.<sup>[19]</sup> The presence of aspartate and/or glutamate residues on the protein surface results in electrostatic interaction in the IMAC method.<sup>[20]</sup> This event may be referred to as mixed mode interactions.

The adsorption properties of the adsorbents were evaluated in terms of the initial equilibrium concentration of  $\alpha$ -amylase (Figure 5B). An increase in the adsorption capacity of the Ni<sup>2+</sup>-N-ACF materials was observed with increasing  $\alpha$ -amylase concentration. After the active sites are completely saturated with  $\alpha$ -amylase molecules, graph for Ni<sup>2+</sup>-N-ACF reached a steady state at the concentration of 3 mg mL<sup>-1</sup>. According to the outcomes, the highest adsorption capacity of Ni<sup>2+</sup>-N-ACF and ACF was calculated as 878.2 and 58.2 mg g<sup>-1</sup> material, respectively.

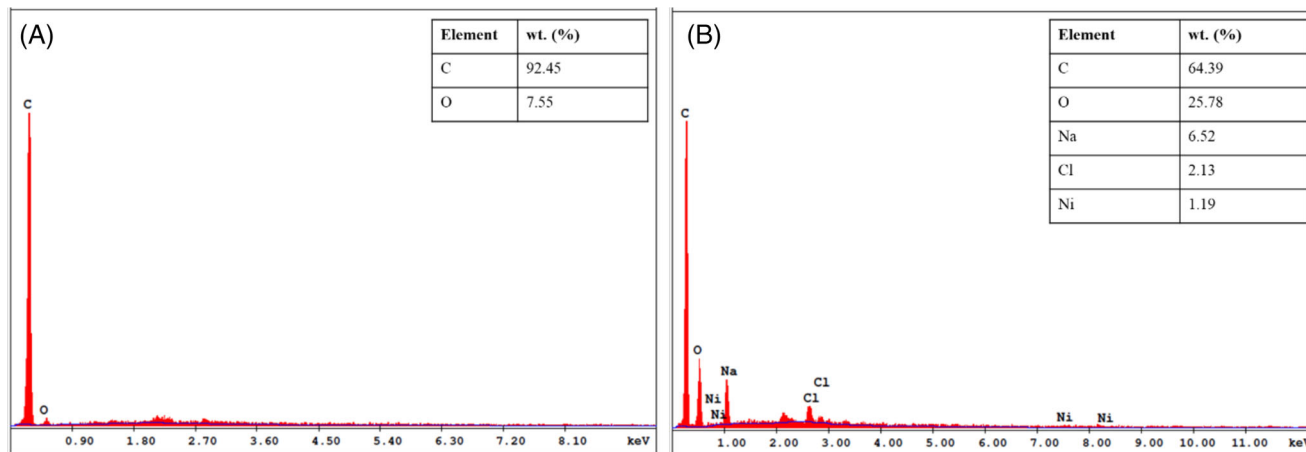


**Figure 3.** Energy dispersive X-ray (EDX) results of (A) null carbon felt and (B) Ni<sup>2+</sup>-N-ACF.

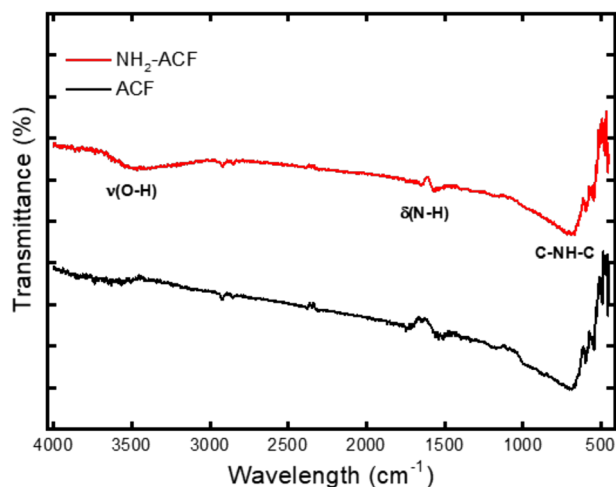


**Figure 4.** FTIR spectra of bare and modified carbon felt (ACF and  $\text{NH}_2$ -ACF).

$\text{Ni}^{2+}$ -N-ACF materials have extremely sufficient adsorption capacity according to ACF.

The impact of ionic strength on  $\alpha$ -amylase adsorption of  $\text{Ni}^{2+}$ -N-ACF was investigated utilizing solutions with different NaCl concentrations (0–1.5 M) as shown in Figure 5C. As seen in the graph,  $\alpha$ -amylase adsorption decreased significantly with increasing NaCl concentration. The main reason for this may be that electrostatic interactions are principally effective for  $\alpha$ -amylase adsorption on the  $\text{Ni}^{2+}$ -N-ACF. With the increase of salt concentration in the environment, it causes the functional groups on the adsorbent and adsorbate to be masked by the coordination of salt ions. This event results in lower adsorption.<sup>[21]</sup> The maximum  $\alpha$ -amylase immobilization on temperature was observed at 25 °C (Figure 5D). After this point, there was a sharp decrease. This may be due to the possibility of the enzyme undergoing a structural change towards higher temperatures.

The reusability of  $\text{Ni}^{2+}$ -N-ACF had an adequate level for further experiments. More than 95% of the  $\alpha$ -amylase adsorbed for this study was observed to be desorbed by 1 M NaCl nearly 20 min. The adsorption–desorption stages were repeated 30 times by working with the same material, and no important change was observed in the construction of the material.

### 3.3. Effect of pH and Temperature on the Activities of the Free and the Immobilized Amylase

Enzyme behavior may be affected by the microenvironment of the enzyme. Optimum pH of an enzyme is generally changed by immobilization process. Effect of pH on enzyme activity was presented in Figure 6. The optimum pH of the immobilized  $\alpha$ -amylase was shifted from pH 7.0 to 5.0. The shift of 2.0 U towards the acidic region due to the immobilization of  $\alpha$ -amylase onto  $\text{Ni}^{2+}$ -N-ACF is natural as the microenvironment of free and immobilized  $\alpha$ -amylase are pretty different. In the study of Aghaei et al.<sup>[22]</sup> and Tüzmen et al.<sup>[23]</sup> optimum pH of  $\alpha$ -amylase had shifted from pH 7.0 to 8.0. The charge and structure of the support material has significant effects on enzyme activity.<sup>[24,25]</sup> As seen in Figure 6, activities of the immobilized  $\alpha$ -amylase at pH

5.0 and 6.0 were quite close values. At pH 7.0 and 8.0, activities of the immobilized  $\alpha$ -amylase were lower than those of the free amylase; however, the immobilized  $\alpha$ -amylase showed adequate activity for starch degradation. Furthermore, activities of the immobilized  $\alpha$ -amylase were detected as 1.77- and 1.46-times higher than that of the free  $\alpha$ -amylase at pH 4.0 and 5.0, respectively. These results proved that  $\alpha$ -amylase immobilized  $\text{Ni}^{2+}$ -N-ACF can be effectively used in acidic media for starch degradation. Atiroğlu et al. determined that  $\alpha$ -amylase immobilized olibanum-bovine serum albumin@zeolitic imidazolate frameworks nanocomposite showed higher activities both at acidic and basic pH regions as compared to the free enzyme.<sup>[25]</sup>

$\alpha$ -Amylase activity increased with increasing temperature up to the optimum temperature (Figure 7). Optimum temperature of the free  $\alpha$ -amylase was determined as 35 °C and that value for the immobilized  $\alpha$ -amylase was shifted to 45 °C. Almulaiky et al. determined that optimum temperature of  $\alpha$ -amylase immobilized both onto hydroxyapatite and onto hydroxyapatite zirconia (10%) nanocomposite had shifted towards higher temperature values (50 °C for free amylase, 60 °C for immobilized amylases).<sup>[26]</sup> The immobilized  $\alpha$ -amylase showed by 1.37- and 1.22-fold higher catalytic activity than that of the free  $\alpha$ -amylase at 45 and 55 °C, respectively. Furthermore, same effect was detected at catalytic activity at low temperature values (1.37-fold for 5 °C, 1.22-fold for 15 °C). Higher catalytic activity of the immobilized  $\alpha$ -amylase as compared to that of the free  $\alpha$ -amylase in a broad temperature range should be advantage for industrial uses.

### 3.4. Kinetic Parameters

Kinetic parameters were identified for the free and the immobilized  $\alpha$ -amylase and results were presented in Table 1. As shown in Table 1,  $V_{\text{max}}$  of the free and the immobilized  $\alpha$ -amylase were pretty close values. This proved that immobilization did not change the maximum velocity of the amylase.  $K_M$  value increased 2.75-fold by immobilization. This increase indicated the reduction in the affinity of enzyme to its substrate by immobilization of  $\alpha$ -amylase onto  $\text{Ni}^{2+}$ -N-ACF.  $K_{\text{cat}}$  is turnover number, expressed as number of substrate molecules turned into product per enzyme per minute.  $K_{\text{cat}}$  and  $K_{\text{cat}}/K_M$  values are practical parameters for the comparison of catalytic efficiency.<sup>[27]</sup> Both  $K_{\text{cat}}$  and  $K_{\text{cat}}/K_M$  values were decreased by immobilization. These results may be explained by steric hindrance, conformational changes, and also microenvironment change.<sup>[28]</sup>

### 3.5. Storage and Operational Stabilities

Storage stabilities of the free and the immobilized  $\alpha$ -amylase were identified for 30 days and results were presented in Figure 8 as relative activities. As shown in Figure 8, the relative activities of the free and the immobilized  $\alpha$ -amylase were determined as similar after 20 days' storage. After 20 days, the relative activity of the free  $\alpha$ -amylase decreased sharply. At the end of 30 days, the immobilized  $\alpha$ -amylase preserved its 59.8% of its initial activity while the free  $\alpha$ -amylase consumed all activity. Almulaiky et al. indicated that free  $\alpha$ -amylase and  $\alpha$ -amylase immobilized on hydroxyapatite (HA) and hydroxyapatite-decorated  $\text{ZrO}_2$  (HA- $\text{ZrO}_2$ )

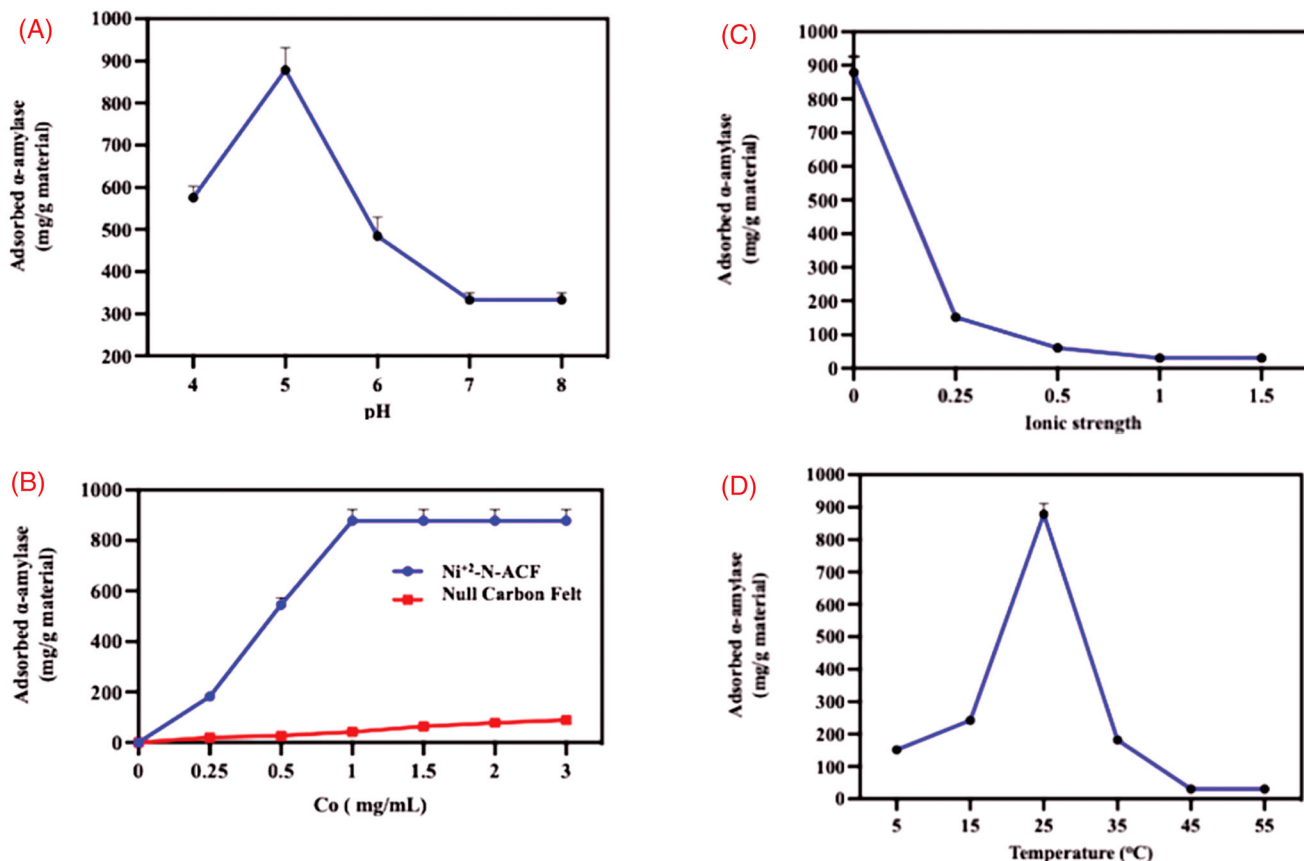


**Figure 5.** A) pH effect on  $\alpha$ -amylase adsorption onto  $\text{Ni}^{2+}$ -N-ACF, B)  $\alpha$ -amylase concentration effect on adsorption onto  $\text{Ni}^{2+}$ -N-ACF, C) ionic strength effect on  $\alpha$ -amylase adsorption onto  $\text{Ni}^{2+}$ -N-ACF, and D) temperature effect on  $\alpha$ -amylase adsorption onto  $\text{Ni}^{2+}$ -N-ACF.

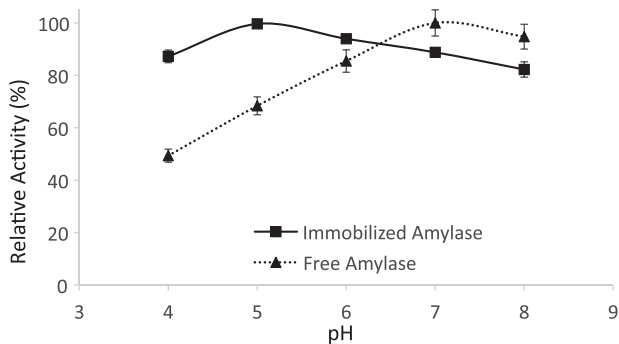


**Figure 6.** pH profiles for the free and the immobilized amylase.

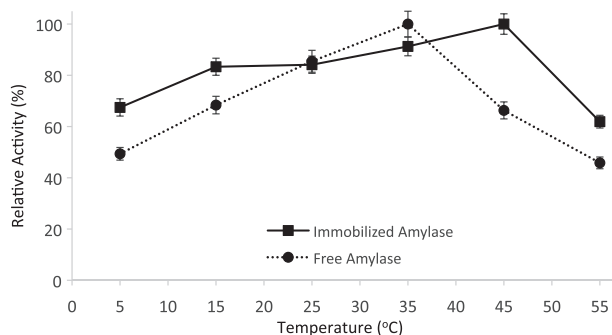


**Figure 7.** Temperature profiles for the free and the immobilized amylase.

**Table 1.** Kinetic parameters for the free and the immobilized amylase.

	$V_{\max}$ [ $\mu\text{mol min}^{-1}$ ]	$K_M$ [ $\text{g L}^{-1}$ ]	$K_{\text{cat}}$	$K_{\text{cat}}/K_M$
Free $\alpha$ -amylase	1.179	1.253	$2.28 \times 10^3$	0.6214
Immobilized $\alpha$ -amylase	1.129	3.442	$2.62 \times 10^2$	0.0261

showed 27%, 50%, and 69% of the remaining enzyme activity after 8 weeks, respectively.<sup>[26]</sup>

$\alpha$ -Amylase activity assay was repeated 15-times to specify the operational stability of the  $\alpha$ -amylase immobilized  $\text{Ni}^{2+}$ -N-ACF (Figure 9). At the second activity assay, a decrease by 18.3% of initial activity was determined. This result may be explained by leakage of the  $\alpha$ -amylase which is immobilized by non-specific interactions. At the end of 15 activity runs,  $\alpha$ -amylase immobilized  $\text{Ni}^{2+}$ -NH<sub>2</sub>-ACF showed 61.0% of its initial activity. Decomposition of  $\text{Ni}^{2+}$ -N-ACF and denaturation of  $\alpha$ -amylase may cause to this decrease. Aghaei et al. determined that the rela-

tive activities of immobilized  $\alpha$ -amylase on cloisite 30B, on epoxy functionalized cloisite, and on tosylated cloisite were 35.9%, 66.4%, and 79.7% after 10 cycles, respectively.<sup>[22]</sup> Baysal et al. and Mohamed et al. proved that  $\alpha$ -amylase immobilized onto chitosan-bentonite hybrid and PPyAgNp/ $\text{Fe}_3\text{O}_4$  nanocomposite

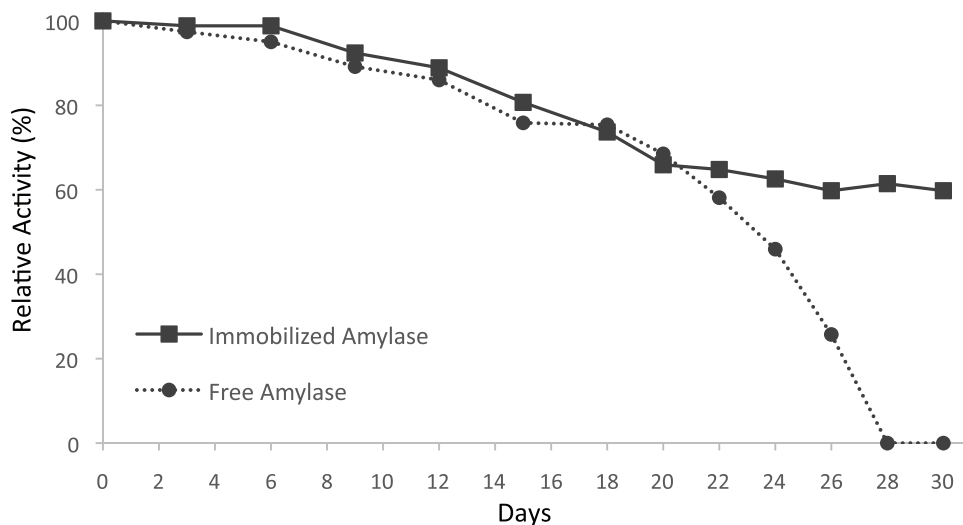


**Figure 8.** Storage stabilities of the free and the immobilized amylase.

showed 87% and 80% of retained activity after 5- and 10-cycles, respectively.<sup>[29,30]</sup> In the study of Tiarsa et al.,  $\alpha$ -amylase immobilized onto chitin-bentonite hybrid preserved 38% of residual activity after 6-cycles.<sup>[31]</sup>

### 3.6. Starch Degradation in Real Potato Wastewater

Potato waste water obtained from fabric was mixed with  $\alpha$ -amylase immobilized  $\text{Ni}^{+2}$ -N-ACF and free  $\alpha$ -amylase (same amount of  $\alpha$ -amylase with immobilized onto  $\text{Ni}^{+2}$ -N-ACF). Amount of released maltose was measured by DNSA method at different time intervals till 24 h. Maltose released after 10- and 30-min incubation by  $\alpha$ -amylase immobilized  $\text{Ni}^{+2}$ -N-ACF were determined as negligible amounts and very close with that by the free amylase. At the end of 24 h incubation, maltose released

by  $\alpha$ -amylase immobilized  $\text{Ni}^{+2}$ -N-ACF was calculated as 7.07-times higher as compared to that by free  $\alpha$ -amylase. This result proved that  $\alpha$ -amylase immobilized  $\text{Ni}^{+2}$ -N-ACF should be used for starch degradation in industrial usage.

## 4. Conclusion

This article presents a new design of  $\text{Ni}^{+2}$ -N-ACFs produced for use in enzyme immobilization, which has many advantages such as time economy, high stability, useful, highly satisfactory binding ability, and low-cost production. For this aim, ACF structures were prepared with nitrogen modify. Then, the samples were characterized by SEM, EDX, and AAS experiments. The maximum adsorption took place at pH 5.0 (878.2 mg  $\text{g}^{-1}$  material). Besides, the reusability experiments were conducted 30

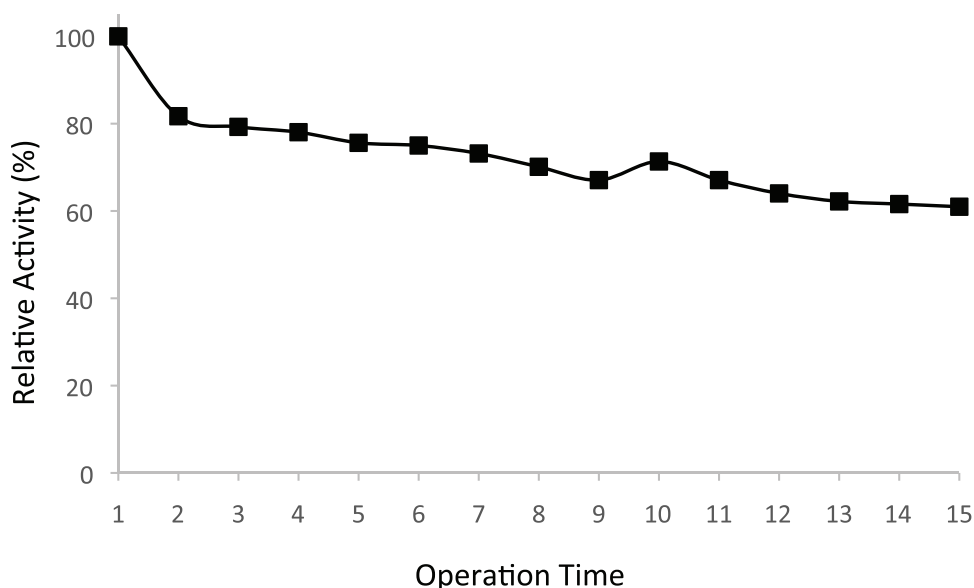


**Figure 9.** Operational stability of the immobilized amylase.

adsorption–desorption cycles with 1 M NaCl for nearly 20 min by utilizing the same material. In addition, the effect of pH and temperature on the activities of the free and the immobilized amylase, kinetic parameters, storage and operational stabilities were determined. The immobilized  $\alpha$ -amylase demonstrated by 1.37- and 1.22-fold higher catalytic activity than that of the free  $\alpha$ -amylase at 45 and 55 °C, respectively. It was observed that the  $V_{\max}$  of free and immobilized  $\alpha$ -amylase were close to each other. This event demonstrates that immobilization does not change the maximum rate of amylase.  $K_M$  value increased by 2.75 times with the immobilization. The increase seen here proves that the immobilization of  $\alpha$ -amylase on Ni<sup>2+</sup>-N-ACF decreases the affinity of the enzyme to its substrate. At the end of 15 activity runs,  $\alpha$ -amylase immobilized Ni<sup>2+</sup>-N-ACF showed 61.0% of its initial activity. The results obtained are comparable with the literature. Lastly, starch degradation in real potato wastewater revealed that Ni<sup>2+</sup>-N-ACFs can be operated for starch degradation. This study is designed to eliminate the limitations such as some difficulties, loss of time, and high cost in some chemical processes.

## Acknowledgements

This research received no external funding.

## Conflict of Interest

The authors declare no conflict of interest.

## Author Contributions

Conceptualization: Ö.A., B.Ö.A., and T.İ.; methodology: E.O.K., B.S.; investigation: N.D., K.O., and M.O.; writing – original draft preparation: K.O., Ö.A., and T.İ.; writing – review and editing: N.D., K.O., and M.O. All authors have read and agreed to the published version of the manuscript.

## Data Availability Statement

The data that support the findings of this study are available from the corresponding author upon reasonable request.

## Keywords

activated carbon felt, activation, alpha-amylase, immobilization, starch degradation

Received: February 3, 2023

Revised: June 25, 2023

Published online: August 24, 2023

- [1] P. R. Yaashikaa, M. K. Devi, P. S. Kumar, *Chemosphere* **2022**, 299, 134390.
- [2] S. Kalia, A. Bhattacharya, S. K. Prajapati, A. Malik, *Chemosphere* **2021**, 279, 130554.
- [3] S. Dhindwal, L. Gomez-Gil, D. B. Neau, T. T. M. Pham, M. Sylvestre, L. D. Eltis, J. T. Bolin, P. Kumar, *J. Bacteriol.* **2016**, 198, 1499.
- [4] A. Arora, S. Priya, P. Sharma, S. Sharma, L. Nain, *Biocatal. Agric. Biotechnol.* **2016**, 8, 66.
- [5] S. Sen, M. Dehingia, N. C. Talukdar, M. Khan, *Sci. Rep.* **2017**, 7, 44406.
- [6] K. Mojsov, *J. Textile Instit.* **2019**, 110, 1032.
- [7] J. S. Paul, N. Gupta, E. Beliya, S. Tiwari, S. K. Jadhav, *Appl. Biochem. Biotechnol.* **2021**, 193, 2649.
- [8] M. Odabaşı, L. Uzun, G. Baydemir, N. H. Aksoy, Ö. Acet, D. Erdönmez, *Colloids Surf. B Biointerfaces* **2018**, 163, 266.
- [9] A. Serinbaş, B. Önal, Ö. Acet, N. Özdemir, V. Dzmirutuk, I. Halets-Bui, D. Shcharbin, M. Odabaşı, *Mater. Sci. Eng., C* **2020**, 113, 111020.
- [10] B. Önal, Ö. Acet, R. Sanz, E. S. Sanz-Pérez, D. Erdönmez, M. Odabaşı, *Int. J. Biol. Macromol.* **2019**, 141, 1183.
- [11] Ö. Acet, N. H. Aksoy, D. Erdönmez, M. Odabaşı, *Artif. Cells Nanomed. Biotechnol.* **2018**, 46, 538.
- [12] J. Porath, J. Carlsson, I. Olsson, G. Belfrage, *Nature* **1975**, 258, 598.
- [13] Ö. Acet, B. Önal, R. Sanz, E. S. Sanz-Pérez, D. Erdönmez, M. Odabaşı, *J. Mol. Liq.* **2019**, 276, 480.
- [14] Ö. Acet, T. İnanan, B. Ö. Acet, E. Dikici, M. Odabaşı, *Appl. Biochem. Biotechnol.* **2021**, 193, 2483.
- [15] P. Bernfeld, *Methods Enzymol.* **1955**, 1, 149.
- [16] T. İnanan, *LWT* **2022**, 154, 112608.
- [17] R. A. Sheldon, *Adv. Synth. Catal.* **2007**, 349, 1289.
- [18] S. N. Freer, *Appl. Environ. Microbiol.* **1993**, 59, 1398.
- [19] M. Zachariou, M. T. W. Hearn, *Biochemistry* **1996**, 35, 202.
- [20] M. Zachariou, M. T. W. Hearn, *J. Protein Chem.* **1995**, 14, 419.
- [21] J. Sun, Y. Su, S. Rao, Y. Yang, *J. Chromatogr. B* **2011**, 879, 2194.
- [22] H. Aghaei, Z. Mohammadbagheri, A. Hemasi, A. Taghizadeh, *Food Chem.* **2022**, 373, 131425.
- [23] N. Tüzmen, T. Kalburcu, A. Denizli, *J. Mol. Catal. B Enzym.* **2012**, 78, 16.
- [24] N. Hasirci, S. Aksoy, H. Turmturk, *React. Funct. Polym.* **2006**, 66, 1546.
- [25] V. Atiroğlu, A. Atiroğlu, M. Özacar, *Food Chem.* **2021**, 349, 129127.
- [26] Y. Q. Almulaiky, N. M. Khalil, R. M. El-Shishtawy, T. Altalhi, Y. Algamal, M. Aldahri, S. A. Al-Harbi, E. S. Allehyani, M. Bilal, M. M. Mohammed, *Int. J. Biol. Macromol.* **2021**, 167, 299.
- [27] T. İnanan, N. Tüzmen, F. Karipcin, *Int. J. Biol. Macromol.* **2018**, 114, 812.
- [28] N. Tüzmen, T. Kalburcu, A. Denizli, *Process Biochem.* **2012**, 47, 26.
- [29] S. A. Mohamed, M. H. Al-Harbi, Y. Q. Almulaiky, I. H. Ibrahim, H. A. Salah, M. O. El-Badry, A. M. Abdel-Aty, A. S. Fahmy, R. M. El-Shishtawy, *Artif. Cells Nanomed. Biotechnol.* **2018**, 46, 201.
- [30] Z. Baysal, Y. Bulut, M. Yavuz, Ç. Aytakin, *Starch – Stärke* **2014**, 66, 484.
- [31] E. R. Tiarsa, Y. Yandri, T. Suhartati, H. Satria, B. Irawan, S. Hadi, *Biochem. Res. Int.* **2022**, 2022, 1.